A

MGG79 (*IDH1*^{R132H})

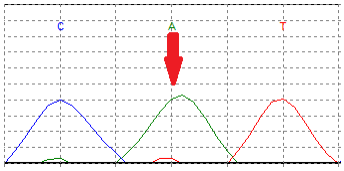

MGG119 (*IDH1*^{R132H})

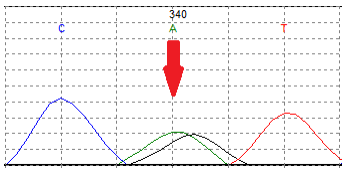

MGG132 (*IDH1*^{R132H})

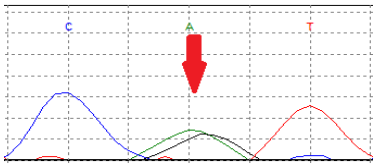

MGG152 (*IDH1*^{R132H})

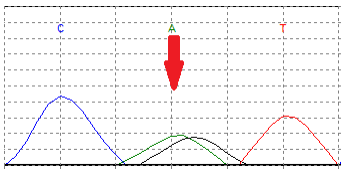

MGG172 (*IDH1*^{R132H})

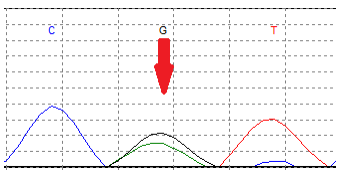

BT142 (*IDH1*^{R132H})

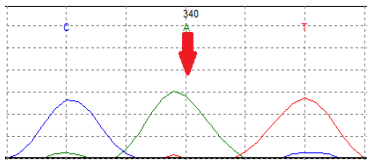

HT1080 (*IDH1*^{R132C})

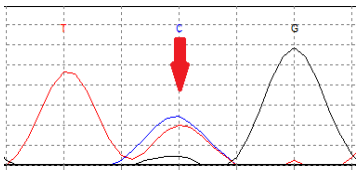

30T (*IDH1*^{R132C})

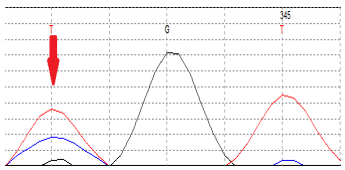

SW1353 (*IDH2*^{R172S})

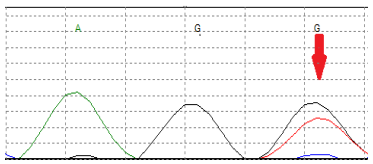

B

MGG119

Brain tumor tissue

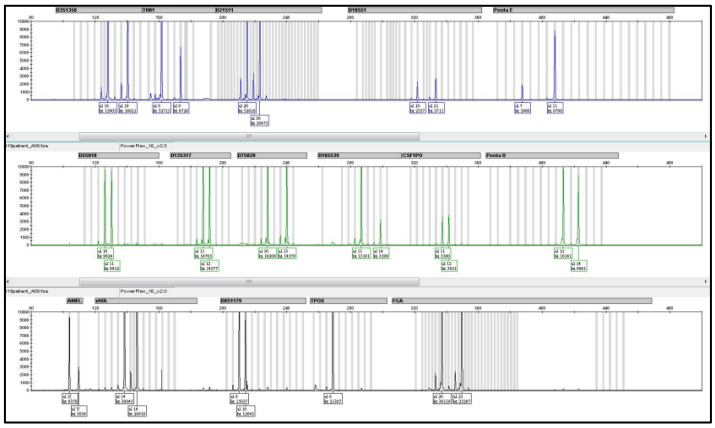

TIC tumorshpheres

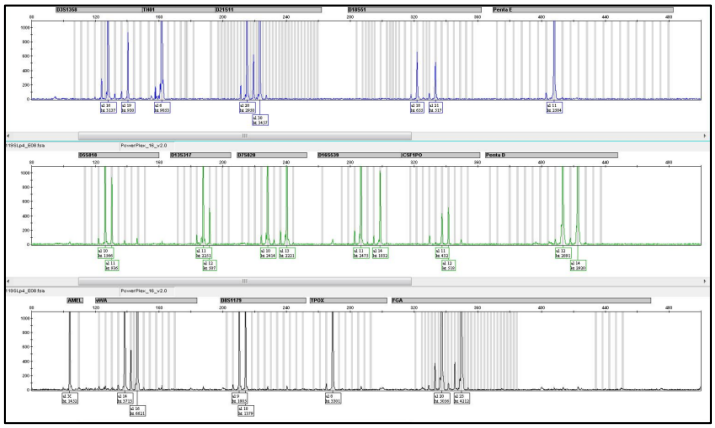

TIC tumorshpheres
with IDH1i 6M

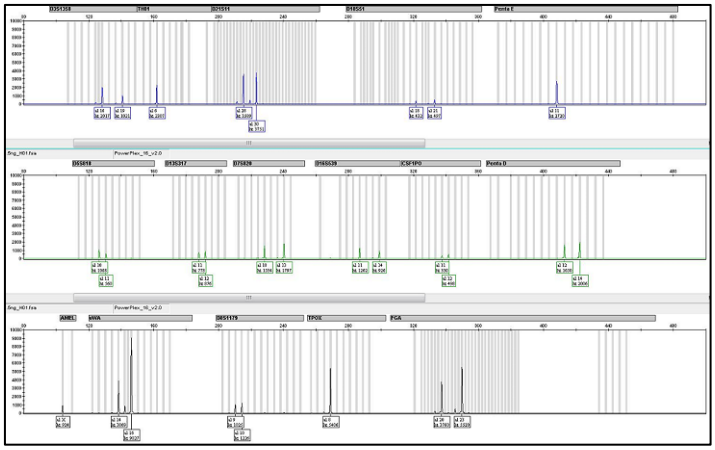

MGG152

Brain tumor tissue

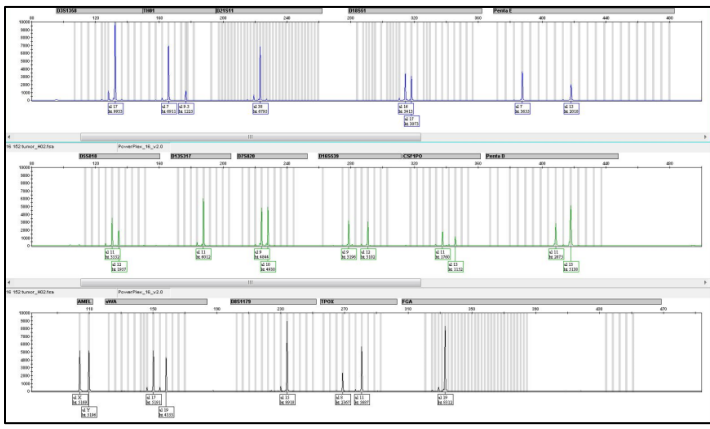

TIC tumorspheres

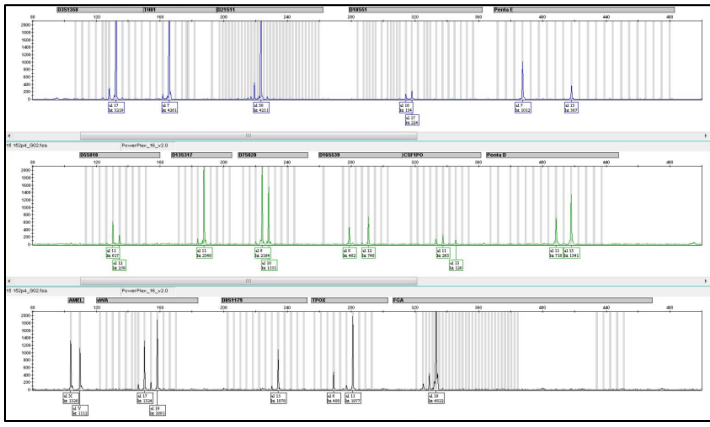

TIC tumorshpheres
with IDH1i 12M

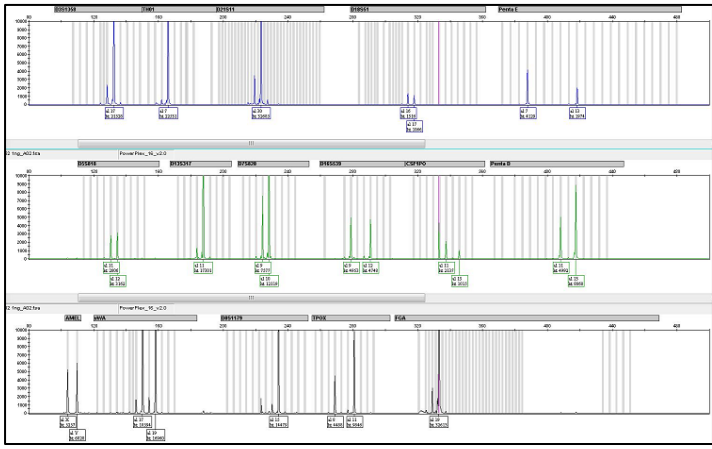

C

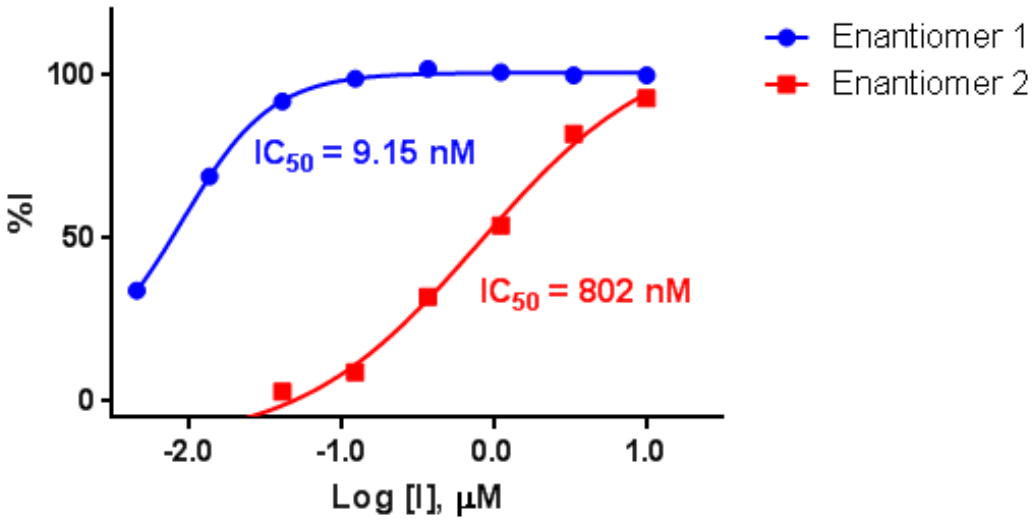
Enantiomer 1
Enantiomer 2
100
50
0
%I
IC50 = 9.15 nM
IC50 = 802 nM
-2.0
-1.0
0.0
1.0
Log [I], µM

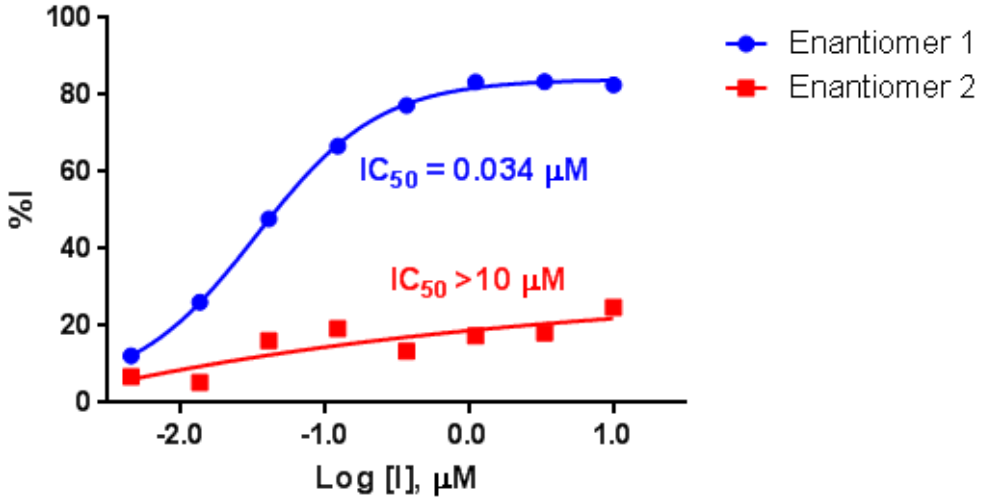
Enantiomer 1
Enantiomer 2
100
80
60
40
20
0
%I
IC50 = 0.034 µM
IC50 >10 µM
-2.0
-1.0
0.0
1.0
Log [I], µM

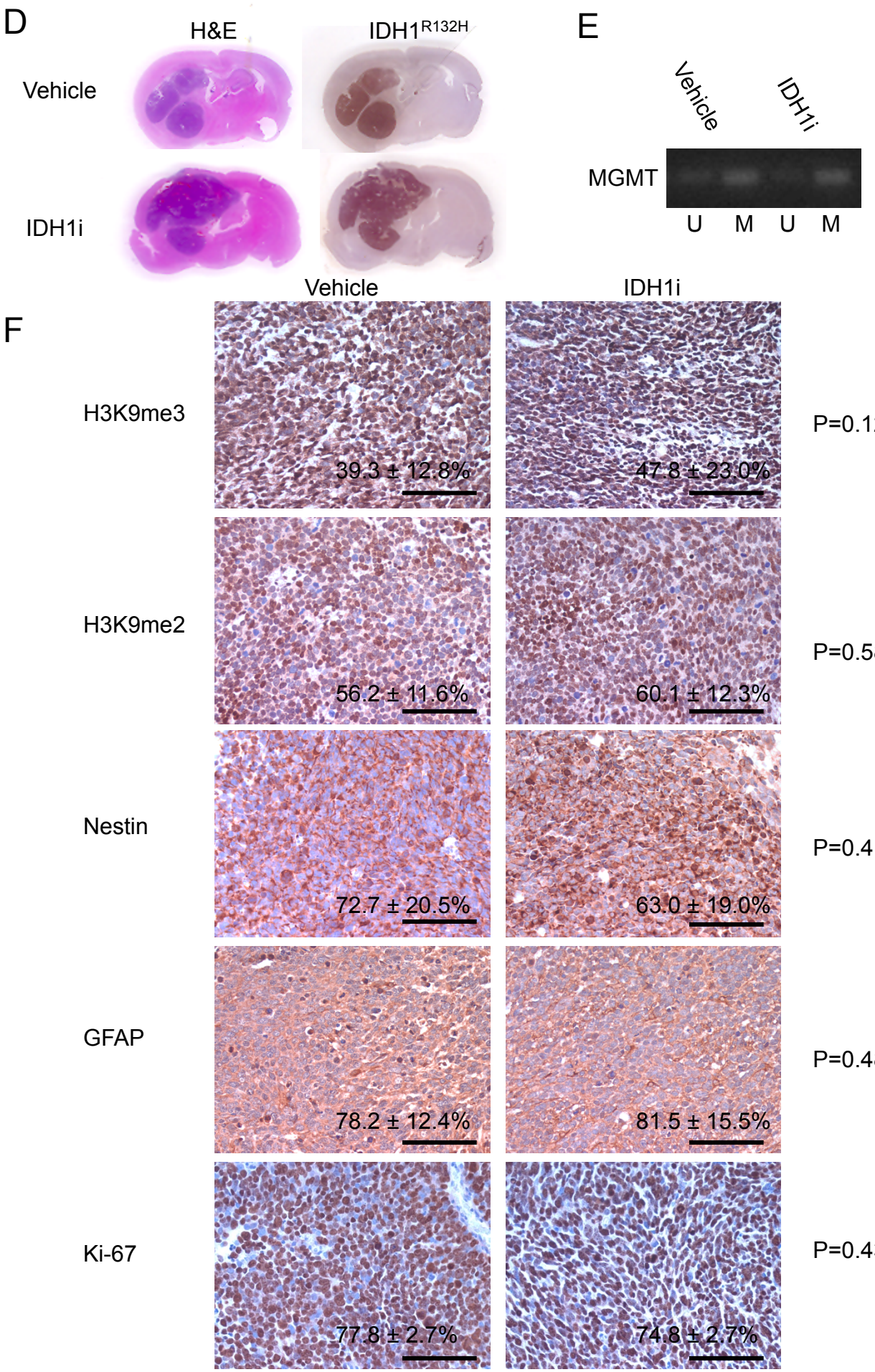
D
H&E
IDH1R132H
Vehicle
IDH1i
E
Vehicle
IDH1i
MGMT
U M U M
F
Vehicle
IDH1i
H3K9me3
39.3 ± 12.8%
47.8 ± 23.0%
P=0.12
H3K9me2
56.2 ± 11.6%
60.1 ± 12.3%
P=0.58
Nestin
72.7 ± 20.5%
63.0 ± 19.0%
P=0.41
GFAP
78.2 ± 12.4%
81.5 ± 15.5%
P=0.48
Ki-67
77.8 ± 2.7%
74.8 ± 2.7%
P=0.43

G

MGG119 with IDH1i (3M)

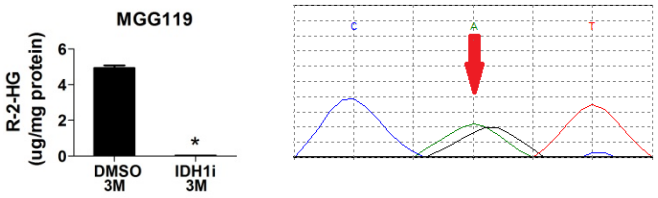

MGG152 with IDH1i (12M)

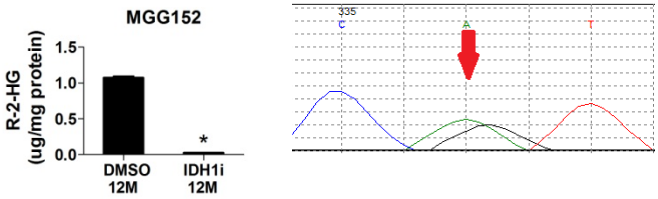

H

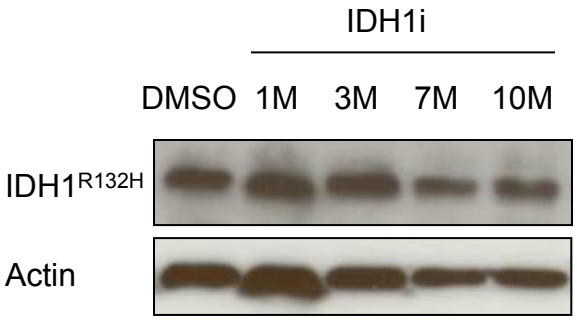

I

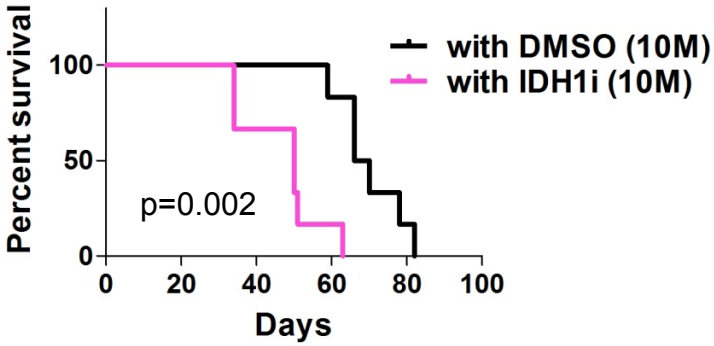

J

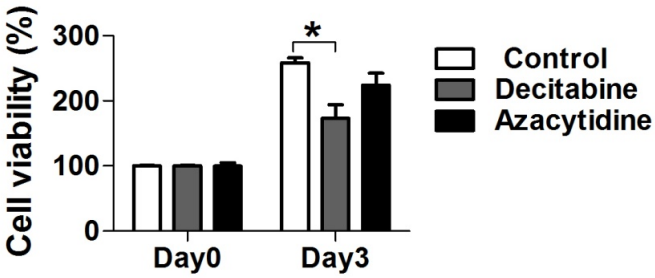

K

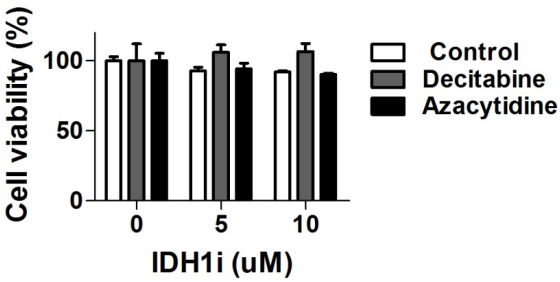

Figure S1, related to Figure 1. *IDH1* mutant genotype and phenotype are retained in Patient-derived *IDH1* mutant glioma TICs and xenografts with short-term and long-term exposure to IDH1i. (A) PCR-based sanger sequence plots of the *IDH1* R132 locus in MGG lines (*IDH1*^{R132H}), BT142 (*IDH1*^{R132H}), HT1080 (*IDH1*^{R132C}), 30T (*IDH1*^{R132C}), and SW1353 (*IDH2*^{R172S}). Red arrow, the interrogated base. (B) Representative genetic fingerprinting data demonstrating matched DNA profiles between patient-derived brain tumor tissue (upper) and corresponding glioma TIC tumorspheres (middle, lower panels) of MGG119 (left panel) and MGG152 (right panel). (C) Biochemical and cellular characterization of IDH1i enantiomers following chiral separation. Top panel, The reductive activity (conversion of aKG to 2-HG) of R132H IDH1 was measured by LC-MS/MS. Peak area of 2-HG was normalized using the peak area of the internal standard $^{13}C_5$-2-HG. Percentage of 2-HG inhibition: %I = 100 x (1-(initial velocity in the presence of compound – background velocity)/(initial velocity in the absence of compound – background velocity). Data were fitted to 4-parameter logistic nonlinear regression model to obtain IC_{50} values. Bottom panel, R132H IDH1-expressing HEK-293 cells were treated with compound or DMSO (final DMSO concentration 0.5%) for 24 hr before 20 µL of cell culture supernatant was harvested for 2-HG quantitation by LC-MS/MS. Percentage of 2-HG inhibition: %I = 100 x (1-(amount of 2-HG in compound treated sample/amount of 2-HG in DMSO-treated sample)). Data were fitted to 4-parameter logistic nonlinear regression model to obtain IC50 values. (D) Mouse MGG152 orthotopic xenografts, coronal sections of whole brain, after hematoxylin and eosin staining (left panel) and IDH1^{R132H} immunohistochemical (IHC) staining (right panel). (E) *MGMT* promotor methylation status of MGG152 orthotopic

xenografts from mice treated with vehicle or IDH1i for 42 days. (F) IHC analysis of H3K9me3, H3K9me2, Nestin, GFAP, and Ki-67 in MGG152 orthotopic xenografts from mice treated with either vehicle (left panels) or IDH1i (right panels) for 42 days. Scale bars, 100 μm. (G) Prolonged exposure of IDH1 inhibitor effect on R-2-HG levels (left panel) in *IDH1* mutant glioma TIC tumorspheres. Genomic PCR-based sequencing of the mutant and wild-type *IDH1* alleles (right panels). (H) Western blot analysis of MGG152 of $IDH1^{R132H}$ protein expression after prolonged exposure to IDH1i. (I) Kaplan-Meier estimates of mouse survival by implantation of MGG152 with prolonged exposure to DMSO or IDH1i. SCID mice were implanted orthotopically (intracerebrally) with $1x10^5$ MGG152 cells that were incubated for 10 months with either IDH1i (pink) or DMSO (black). (J) 3-day cell viability assay of MGG152 pretreated with DMSO, decitabine (1 μM) or azacytidine (1 μM) for 1month. Data were normalized to Day 0. (K) Cell viability assay of MGG152 after 72 hour treatment with DMSO, decitabine (1 μM) or azacytidine (1 μM) +/- IDH1i (5 μM). Cells were incubated with these compounds for 1month prior to measuring cell viability. Data were normalized to those without IDHi.

Table S1, related to Figure 2

Component Name	DMSO-2 days	IDH1i-2 days	DMSO 6 months	IDH1i-6 months	IDH1i/ DMSO 2 days	IDH1i/ DMSO 6 months
1-methylhistamine	**	**	**	**	**	**
2-Aminoadipic acid	6.77E+03	1.17E+04	1.43E+04	9.94E+03	1.73	0.70
2'-deoxyadenosine	1.05E+03	8.48E+02	4.15E+02	3.62E+02	0.81	0.87
2'-deoxycytidine	3.68E+03	4.97E+03	7.11E+02	5.65E+02	1.35	0.79
3-hydroxyanthranilic acid	2.32E+04	2.90E+04	1.90E+04	1.22E+04	1.25	0.64
3-OH-Kynurenic Acid	**	**	**	**	**	**
3-phosphoglyceric acid	**	**	**	**	**	**
4-Hydroxy-3-methoxyphenylglycol	**	**	**	**	**	**
4-hydroxybenzoate	1.47E+03	2.61E+03	6.21E+03	3.73E+03	1.78	0.60
5'-adenosylhomocysteine	3.02E+02	5.68E+02	3.43E+02	4.12E+02	1.88	1.20
5-HIAA	5.06E+02	7.17E+02	2.72E+02	2.04E+02	1.42	0.75
5-Hydroxyindole-3-acetic acid	5.15E+03	6.19E+03	5.73E+03	4.91E+03	1.20	0.86
5-hydroxytryptophan	3.35E+02	7.25E+02	2.77E+02	**	2.16	**
Acetoacetate	1.35E+03	1.52E+03	8.42E+02	1.83E+03	1.13	2.18
acetylcholine	3.45E+03	4.38E+03	1.19E+03	6.45E+02	1.27	0.54
Aconitate	4.64E+04	8.15E+04	7.75E+04	7.02E+04	1.76	0.91
Adenine	2.25E+04	3.23E+04	2.05E+04	1.03E+04	1.43	0.50
adenosine	3.14E+04	6.11E+04	3.36E+04	1.00E+04	1.94	0.30
ADMA/SDMA	4.94E+03	6.10E+03	2.77E+03	2.98E+03	1.23	1.08
alanine	1.71E+05	2.17E+05	1.89E+05	1.13E+05	1.27	0.60
allantoin	2.77E+02	4.30E+02	**	**	1.55	**
alpha-glycerophosphocholine	1.97E+04	1.66E+04	6.20E+02	3.63E+03	0.84	5.85
alpha-keto-glutarate	1.09E+04	1.47E+04	8.41E+03	3.96E+03	1.35	0.47
aminoisobutyric acid	1.41E+03	1.04E+03	8.79E+02	3.03E+02	0.74	0.34
Aminolevulinic acid	2.17E+03	3.16E+03	2.69E+03	2.51E+02	1.46	0.09
anandamide	**	**	**	**	**	**
anserine	**	**	**	**	**	**
anthranilic acid	1.51E+03	2.11E+03	1.78E+03	7.35E+02	1.40	0.41
arginine	1.99E+04	2.33E+04	**	1.76E+04	1.18	**
arginosuccinate	7.74E+02	1.57E+03	9.65E+02	4.47E+02	2.02	0.46
asparagine	2.66E+04	3.27E+04	1.51E+04	1.62E+04	1.23	1.07
aspartate	7.04E+03	8.69E+03	2.29E+04	4.29E+04	1.23	1.87
ATP	**	**	**	**	**	**
beta-alanine	1.26E+05	1.71E+05	1.94E+05	3.09E+04	1.35	0.16
betaine	4.03E+05	5.21E+05	2.07E+05	5.40E+04	1.29	0.26
billirubin	**	**	**	**	**	**
C10-carnitine	**	**	**	**	**	**
C12-carnitine	4.88E+02	7.93E+02	7.65E+02	3.08E+02	1.62	0.40
C14-carnitine	8.38E+03	1.05E+04	1.98E+04	1.00E+04	1.25	0.51
C16-carnitine	3.96E+04	6.11E+04	9.87E+04	4.96E+04	1.54	0.50
C18:1-carnitine	3.65E+04	5.71E+04	5.24E+04	4.08E+04	1.56	0.78
C18:2-carnitine	3.63E+03	5.78E+03	3.84E+03	2.18E+03	1.59	0.57
C18-carnitine	2.23E+04	3.07E+04	1.52E+04	7.30E+03	1.38	0.48
C24:4-carnitine	**	**	**	**	**	**
C26-carnitine	**	**	**	**	**	**

C2-carnitine	1.09E+06	1.43E+06	2.96E+05	7.57E+04	1.31	0.26
C3-carnitine	1.47E+04	1.90E+04	2.40E+04	1.66E+04	1.29	0.69
C3-malonyl-carnitine	2.71E+04	3.33E+04	7.89E+03	1.93E+03	1.23	0.24
C4-butyryl-carnitines	4.10E+04	5.37E+04	5.51E+04	4.90E+04	1.31	0.89
C4-methylmalonyl-carnitine	5.69E+02	1.30E+03	7.10E+02	1.02E+03	2.29	1.43
C5-glutaryl-carnitine	**	**	**	**	**	**
C5-valeryl-carnitines	3.67E+03	6.93E+03	1.60E+04	1.95E+04	1.89	1.22
C6-carnitine	1.84E+03	1.94E+03	2.66E+03	1.02E+03	1.05	0.38
C7-carnitine	1.79E+02	3.08E+02	2.14E+02	1.57E+02	1.72	0.73
C8-carnitine	3.30E+02	**	**	**	**	**
C9-carnitine	**	**	**	**	**	**
cAMP	**	**	5.73E+02	**	**	**
carnitine	9.37E+04	1.30E+05	1.26E+05	3.26E+04	1.39	0.26
carnosine	**	**	**	**	**	**
cGMP	**	**	**	**	**	**
choline	1.62E+06	1.94E+06	1.23E+06	5.06E+05	1.20	0.41
cis/trans hydroxyproline	1.58E+03	9.96E+02	8.28E+02	2.05E+03	0.63	2.48
citicholine	2.22E+03	3.59E+03	3.90E+03	3.74E+03	1.62	0.96
Citric Acid	**1.12E+05**	**2.17E+05**	**3.08E+05**	**5.17E+05**	**1.93**	**1.68**
Citrulline	9.57E+02	4.52E+03	4.94E+03	3.42E+03	4.72	0.69
cobalamin	**	**	**	**	**	**
cotinine	**	**	**	**	**	**
creatine	9.86E+05	1.21E+06	2.20E+05	1.21E+05	1.23	0.55
creatinine	**	**	**	**	**	**
cystamine	**	**	**	**	**	**
cysteamine	**	**	1.79E+02	**	**	**
cytidine	5.47E+03	9.08E+03	8.53E+03	1.06E+04	1.66	1.25
cytosine	4.90E+02	3.85E+02	8.25E+02	6.91E+02	0.78	0.84
D-alpha-hydroxyglutaric acid	**4.55E+06**	**6.03E+05**	**4.55E+06**	**4.30E+05**	**0.13**	**0.09**
DHAP	1.48E+04	7.77E+04	6.32E+03	7.23E+03	5.26	1.14
Dimethyl-2 oxoglutarate	**	**	**	**	**	**
dimethylglycine	5.38E+04	6.00E+04	3.69E+04	1.71E+04	1.11	0.46
Fructose	2.90E+05	4.01E+05	1.42E+04	7.23E+03	1.38	0.51
fumarate	2.27E+04	4.19E+04	2.19E+05	2.58E+04	1.85	0.12
GABA	7.03E+03	1.17E+04	7.89E+03	2.53E+03	1.66	0.32
Geranyl pyrophosphate	2.69E+03	4.62E+03	6.08E+03	4.55E+03	1.72	0.75
glucose	4.86E+02	5.76E+02	1.74E+02	**	1.19	**
glutamate	2.22E+05	3.54E+05	3.20E+05	3.05E+05	1.59	0.95
glutamine	1.22E+06	1.42E+06	2.38E+04	4.18E+04	1.17	1.75
Glyceraldehyde	4.54E+03	4.44E+03	1.22E+03	1.20E+03	0.98	0.98
glycerol	1.07E+02	1.78E+02	2.67E+02	8.01E+01	1.67	0.30
Glycerol-3-P	**1.90E+04**	**4.50E+04**	**1.94E+04**	**5.61E+04**	**2.36**	**2.89**
glycine	3.25E+03	3.45E+03	1.24E+03	1.03E+03	1.06	0.83
GMP	3.14E+03	6.80E+03	7.61E+03	7.69E+03	2.17	1.01
GTP	**	**	**	**	**	**
Hippuric Acid	**	**	**	**	**	**
histamine	5.52E+03	7.38E+03	1.22E+04	6.00E+03	1.34	0.49
histidine	6.36E+04	9.30E+04	4.25E+04	3.28E+04	1.46	0.77
homocysteine	**	**	**	**	**	**

Homogentistic acid	4.25E+03	6.08E+03	1.11E+04	7.76E+03	1.43	0.70
hypoxanthine	7.43E+04	1.05E+05	5.77E+04	4.18E+04	1.41	0.72
IMP	3.81E+03	1.09E+04	5.28E+03	6.36E+03	2.86	1.21
Inosine	2.80E+04	5.23E+04	3.42E+04	2.30E+04	1.87	0.67
Inositol	3.26E+02	1.38E+03	1.25E+03	8.14E+02	4.24	0.65
isoleucine	2.80E+05	3.88E+05	1.12E+05	8.14E+04	1.39	0.73
kynurenic acid	**	**	**	**	**	**
kynurenine	2.13E+02	7.67E+02	4.18E+02	3.60E+02	3.60	0.86
Lactic Acid	2.54E+05	3.04E+05	5.40E+04	2.41E+04	1.20	0.45
Lactose	1.48E+03	2.57E+03	1.49E+03	7.21E+02	1.73	0.48
leucine	4.16E+05	5.45E+05	1.10E+05	8.60E+04	1.31	0.78
lysine	2.95E+04	4.67E+04	1.55E+04	1.35E+04	1.58	0.87
Malic acid	1.32E+06	1.96E+06	9.04E+05	1.39E+06	1.48	1.54
Malonate	1.81E+04	2.09E+04	6.84E+03	3.91E+03	1.15	0.57
methionine	1.21E+04	1.44E+04	**	5.59E+03	1.19	**
methyl-hydroxyisobutyric acid	**	**	**	**	**	**
Mevalonate	**	**	**	**	**	**
NADH	**3.41E+02**	**2.73E+03**	**4.40E+02**	**1.11E+03**	**8.00**	**2.53**
N-carbomoyl-beta-alanine	1.06E+04	1.27E+04	2.36E+03	4.69E+03	1.20	1.99
niacinamide	2.95E+05	3.69E+05	4.47E+05	2.83E+05	1.25	0.63
Nicotinic Acid	4.71E+03	6.05E+03	2.84E+03	9.61E+02	1.29	0.34
NMMA	9.07E+01	3.33E+02	4.14E+01	4.60E+01	3.67	1.11
OH-phenyl pyruvate	6.97E+02	6.44E+02	1.19E+02	**	0.92	**
ornithine	2.48E+03	2.12E+03	1.10E+03	2.02E+03	0.85	1.84
Orotic acid	5.06E+03	7.28E+03	5.03E+03	5.67E+03	1.44	1.13
oxalic acid	4.05E+03	7.47E+03	2.93E+03	3.51E+03	1.85	1.20
Oxaloacetate	6.99E+03	6.50E+03	8.97E+03	9.97E+03	0.93	1.11
Pantothenic acid	7.13E+04	1.46E+05	1.38E+05	1.62E+05	2.05	1.17
PGE2	**	**	**	**	**	**
phenylalanine	7.28E+05	1.02E+06	3.51E+05	2.32E+05	1.40	0.66
phosphocholine	1.18E+05	1.37E+05	1.40E+05	9.75E+04	1.17	0.70
phosphoethanolamine	3.06E+04	2.98E+04	3.07E+04	2.96E+04	0.97	0.97
Phosphotyrosine	9.00E+03	1.88E+04	9.52E+03	8.61E+03	2.09	0.90
proline	1.48E+06	1.93E+06	1.24E+06	1.18E+06	1.30	0.96
propanoic acid	**	**	**	**	**	**
Protoporphyrin IX	**	**	**	**	**	**
Pyruvate	**	**	**	**	**	**
Quinollininc acid	**	**	**	**	**	**
serine	8.03E+04	9.71E+04	3.59E+04	2.25E+04	1.21	0.63
serotonin	**	**	**	**	**	**
Sorbitol	3.45E+03	4.91E+03	2.03E+03	2.27E+03	1.42	1.12
spermidine	**	**	**	**	**	**
spermine	1.13E+05	1.81E+05	3.17E+05	2.19E+05	1.60	0.69
Succinate	4.18E+05	5.93E+05	2.75E+05	1.98E+05	1.42	0.72
taurine	8.82E+03	1.01E+04	**	2.52E+03	1.15	**
thiamine	1.09E+06	1.55E+06	1.73E+05	1.14E+05	1.43	0.66
threonine	1.91E+05	2.46E+05	9.90E+04	6.46E+04	1.29	0.65
thymidine	2.86E+03	2.96E+03	3.08E+02	9.35E+01	1.04	0.30
thyroxine	**	**	2.99E+01	**	**	**

triiodothyronine	**	**	**	**	**	**
trimethylamine-N-oxide	2.28E+03	2.90E+03	2.37E+03	1.40E+03	1.27	0.59
tryptophan	1.63E+05	2.01E+05	7.24E+04	5.91E+04	1.23	0.82
tyrosine	7.20E+04	1.18E+05	3.66E+04	2.39E+04	1.65	0.65
UDP-Glucuronic acid	**	**	**	**	**	**
UMP	1.06E+04	1.98E+04	1.16E+04	1.72E+04	1.87	1.48
Uric Acid	2.69E+02	1.18E+02	1.88E+02	1.90E+02	0.44	1.01
uridine	3.97E+04	6.47E+04	5.66E+04	4.98E+04	1.63	0.88
valine	5.52E+05	6.52E+05	2.78E+05	1.79E+05	1.18	0.64
xanthine	2.03E+03	9.19E+02	2.13E+03	1.53E+03	0.45	0.72
xanthosine	1.23E+04	1.95E+04	1.71E+04	1.23E+04	1.58	0.72
xanthurenate	3.47E+03	4.02E+03	2.55E+03	1.29E+03	1.16	0.51
XMP	2.21E+03	6.98E+03	4.21E+03	4.30E+03	3.15	1.02

**below level of detection

red; ≥1.50, blue; ≤0.50, compared to DMSO control

A

MGG18-Parental

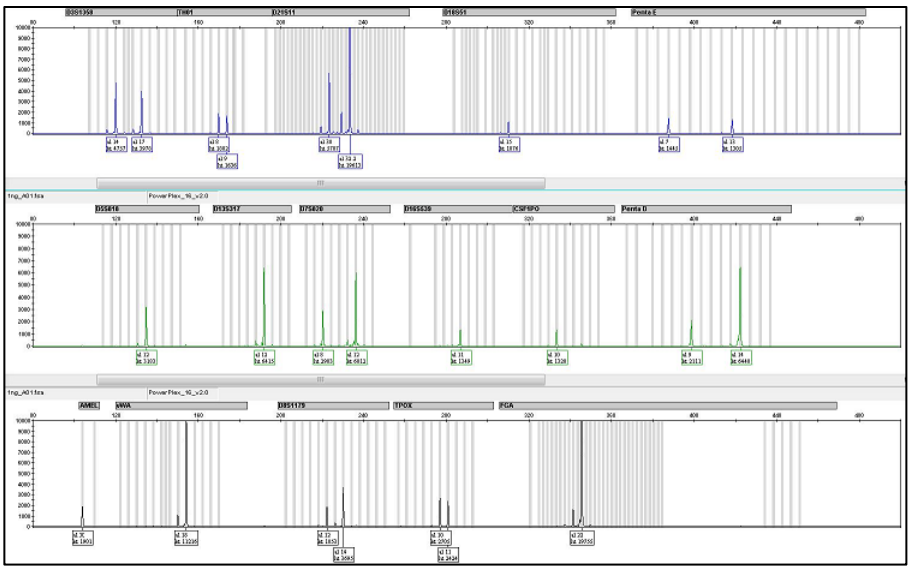

MGG18-IDH1-R132H (tet-)

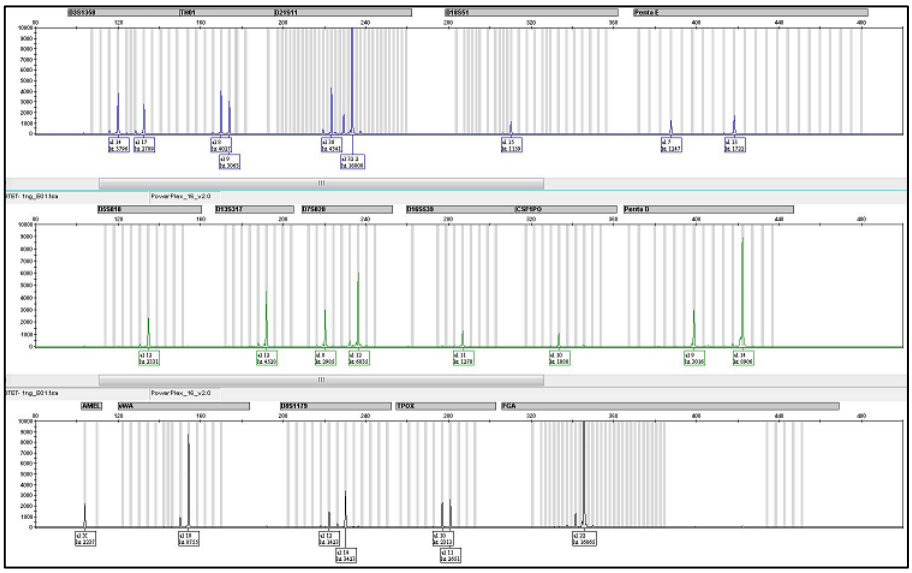

MGG18-IDH1-R132H (tet+)

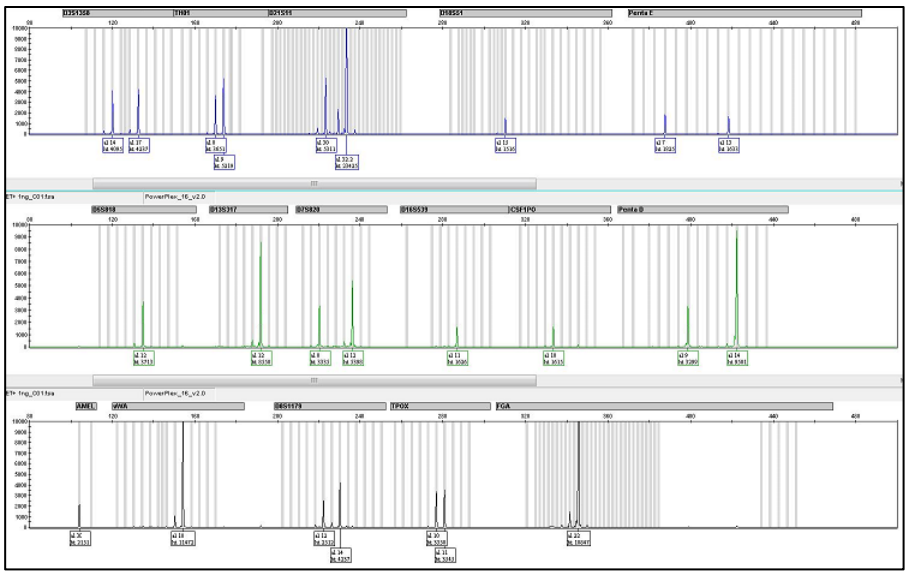

B

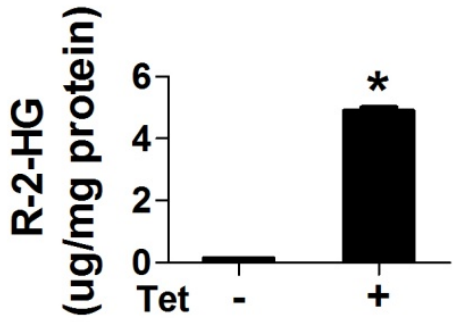
R-2-HG
(ug/mg protein)
6
4
2
0
*
Tet
-
+

C

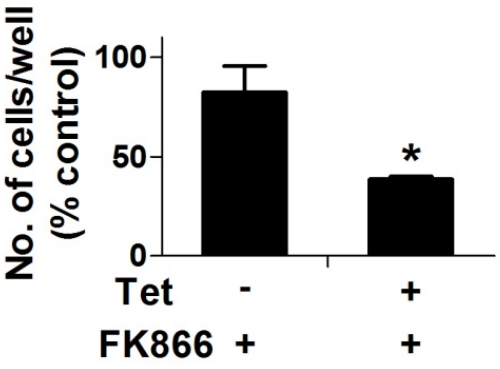
No. of cells/well
(% control)
100
50
0
*
Tet
-
+
FK866
+
+

D

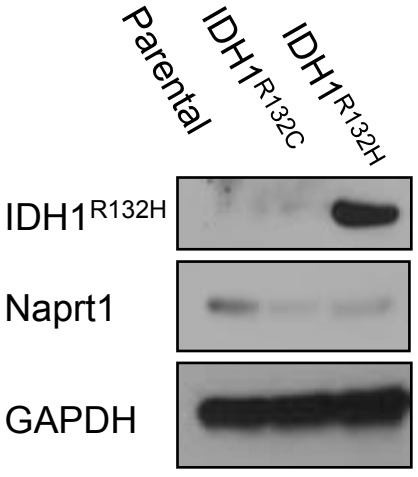
Parental
IDH1R132C
IDH1R132H
IDH1R132H
Naprt1
GAPDH

E

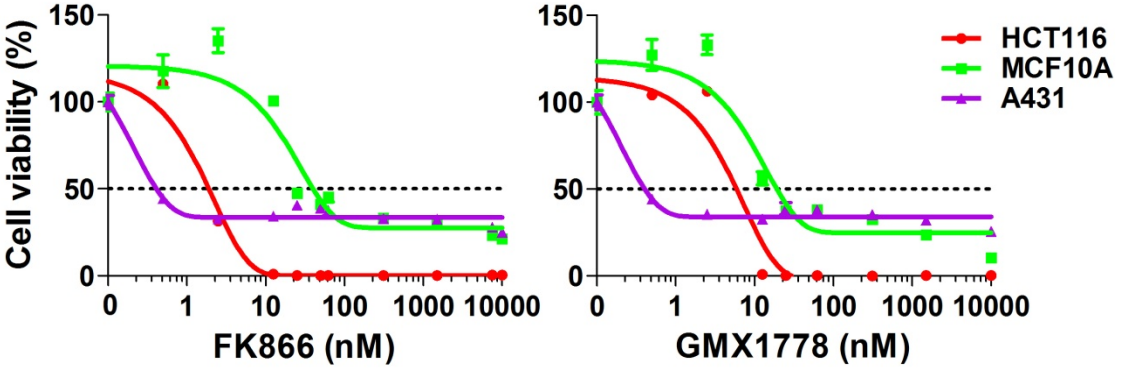
Cell viability (%)
150
100
50
0
0
1
10
100
1000
10000
FK866 (nM)
GMX1778 (nM)
HCT116
MCF10A
A431

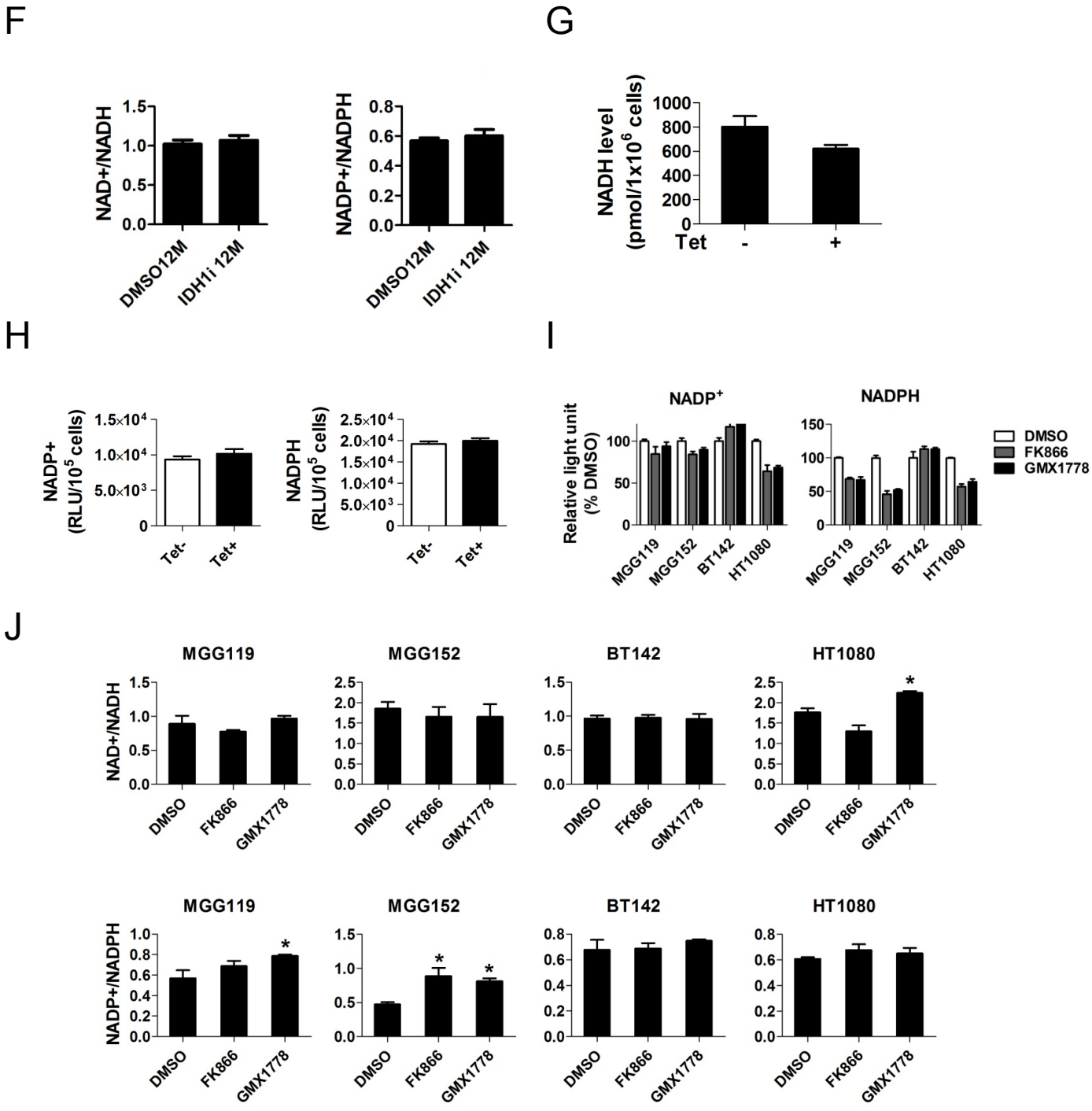
F
NAD+/NADH
1.5
1.0
0.5
0.0
DMSO12M
IDH1i 12M
NADP+/NADPH
0.8
0.6
0.4
0.2
0.0
DMSO12M
IDH1i 12M
G
NADH level (pmol/1x10^6 cells)
1000
800
600
400
200
0
Tet - +
H
NADP+ (RLU/10^5 cells)
1.5×10^4
1.0×10^4
5.0×10^3
0
Tet- Tet+
NADPH (RLU/10^5 cells)
2.5×10^4
2.0×10^4
1.5×10^4
1.0×10^4
5.0×10^3
0
Tet- Tet+
I
NADP+
NADPH
Relative light unit (% DMSO)
100
50
0
150
100
50
0
MGG119 MGG152 BT142 HT1080
DMSO
FK866
GMX1778
J
MGG119
MGG152
BT142
HT1080
NAD+/NADH
1.5
1.0
0.5
0.0
2.5
2.0
1.5
1.0
0.5
0.0
*
DMSO FK866 GMX1778
NADP+/NADPH
1.0
0.8
0.6
0.4
0.2
0.0
1.5
1.0
0.5
0.0
0.8
0.6
0.4
0.2
0.0
*
*
*

Figure S2, related to Figure 4. Effect of NAMPT inhibitors in isogenic mutant *IDH1* cell lines. (A) Representative genetic fingerprinting data of matched DNA profiles between MGG18-parental (upper panel), MGG18-IDH1-R132H (tet^-, middle panel), and MGG18-IDH1-R132H (tet^+, lower panel). (B) Quantitation of R-2-HG in MGG18 (*IDH1/2* wild-type) engineered with a tetracycline (tet)-inducible $IDH1^{R132H}$ gene. (C) Trypan blue exclusion assay of MGG18-IDH1-R132H cells treated with FK866 (12.5 nM) for 8 days +/- 2-month tet induction. Bars, +/-SEM, * $p<0.05$. (D), Western blot analysis of $IDH1^{R132H}$ and Naprt1 in HCT116-Parental, -$IDH1^{R132C}$, and -$IDH1^{R132H}$. GAPDH, loading control. (E) Cell viability assay (CellTiter-Glo) of selected *IDH1/2* wild-type cell lines after 72 hr treatment with FK866 (left panel) and GMX1778 (right panel). HCT116 (colorectal carcinoma), red, MCF10A (breast adenocarcinoma), green, and A431 (lung squamous carcinoma), purple. (F) Ratios of NAD+/NADH and NADP+/NADPH +/- long-term treatment with IDH1 inhibitor in MGG152 cells. (G) NADH levels of MGG18-IDH1-R132H cells +/- tet induction for 2 months. (H) NADP+ (RLU, relative light unit; left panel), and NADPH (right panel) levels of MGG18-IDH1-R132H cells +/- tet induction for 2 months. (I) NAMPT inhibitor effect on NADP+ and NADPH levels in *IDH1* mutant cells *in vitro*. Cells were treated with FK866 (12.5 nM,) or GMX1778 (12.5 nM) for 24 hr prior to measurement. Data are represented as % DMSO control. (J) NAD+/NADH ratio (upper panel) and NADP+/NADPH ratio (lower panel) of *IDH1* mutant cells treated 24 hr with DMSO, FK866 (12.5nM), or GMX1778 (12.5nM). Bars, +/-SEM, * $p<0.05$.

A

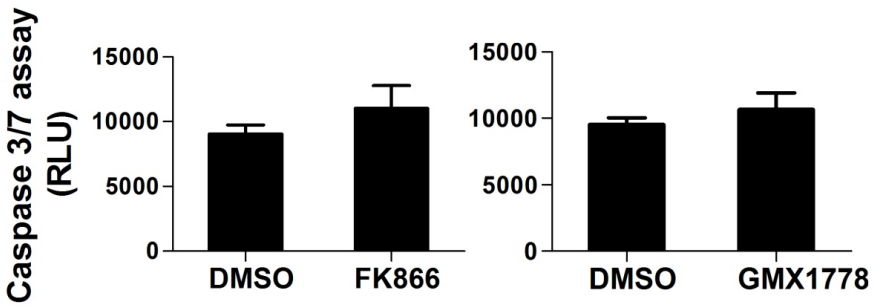
Caspase 3/7 assay (RLU)
15000
10000
5000
0
DMSO
FK866
15000
10000
5000
0
DMSO
GMX1778

B

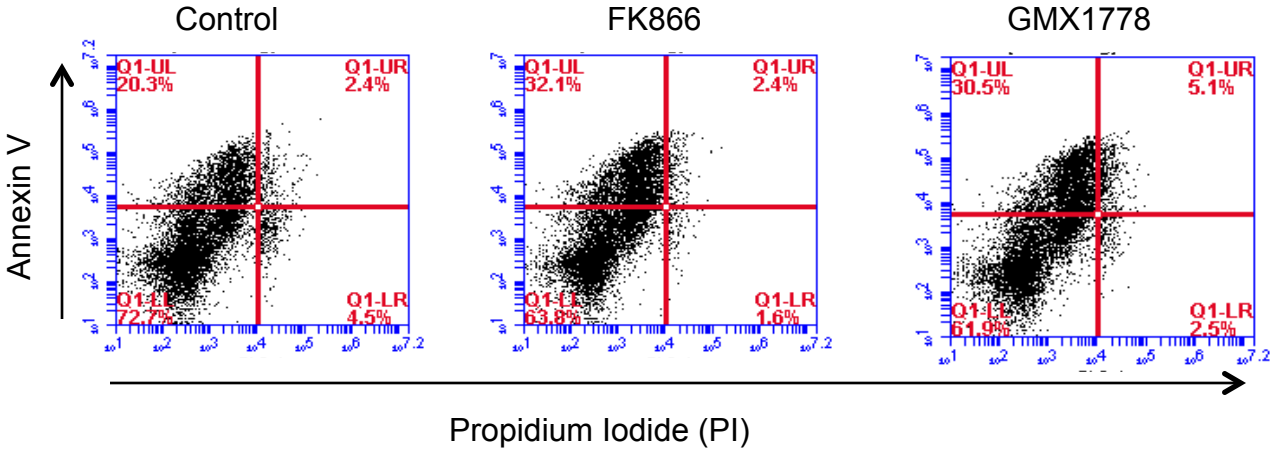
Control
FK866
GMX1778
Annexin V
Q1-UL 20.3%
Q1-UR 2.4%
Q1-LL 72.7%
Q1-LR 4.5%
Q1-UL 32.1%
Q1-UR 2.4%
Q1-LR 1.6%
Q1-UL 30.5%
Q1-UR 5.1%
Q1-LR 2.5%
Propidium Iodide (PI)

Figure S3, related to Figure 6. Apoptosis is not the main mechanism of cell death in *IDH*-mutant cells treated with NAMPT inhibitors. (A) Caspase-Glo 3/7 Assay of MGG152 cells treated for 36 hr with DMSO, FK866 (12.5 nM, left panel), or GMX1778 (12.5 nM, right panel). Data are expressed as relative light unit (RLU). (B) Flow cytometric analysis of MGG152 cells treated with DMSO (left panel), FK866 (12.5 nM, middle panel) or GMX1778 (12.5 nM, right panel) for 48 hr. Fraction of cells positive for Annexin V (Y axis) after FK866 treatment was 32.1%, after GMX1778 treatment 30.5% and after DMSO treatment 20.3%. Fractions of cells positive for propidium iodide (PI) are shown on the X axis.

A

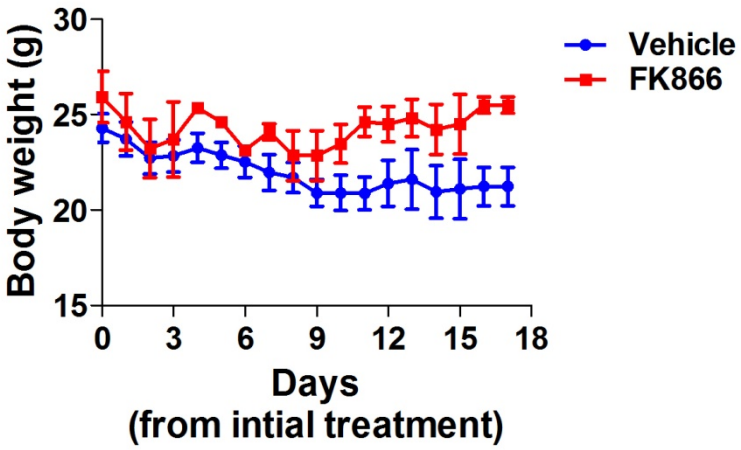
Body weight (g)
30
25
20
15
0
3
6
9
12
15
18
Days
(from intial treatment)
Vehicle
FK866

B

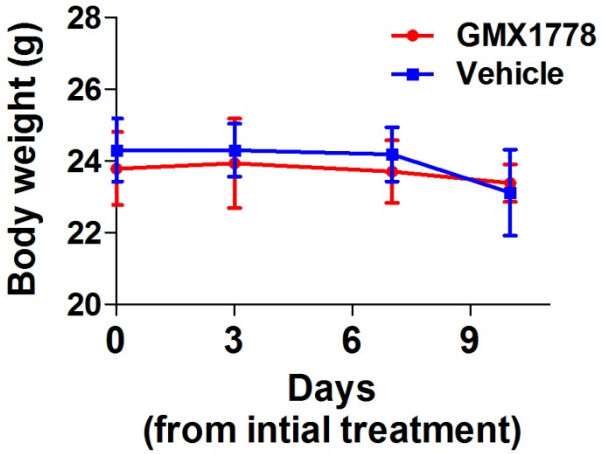
Body weight (g)
28
26
24
22
20
0
3
6
9
Days
(from intial treatment)
GMX1778
Vehicle

Figure S4, related to Figure 7. Nampt inhibitors are tolerated by mice. (A) Body weights of SCID mice harboring HT1080 cells intraperitoneally during oral gavage treatment (4 days/week) with FK866 (30 mg/kg, n=6) or vehicle (n=6). (B) Body weights of SCID mice with intracranial MGG152 cells during oral gavage treatment once per week oral gavage treatment of GMX1778 (250 mg/kg, n=6) or vehicle (n=6). Weights were measured daily (A) or twice per week (B). Bars, +/-SEM.

SUPPLEMENTAL EXPERIMENTAL PROCEDURES

(R)-2-HG quantification using chemical derivatization and LC-SRM MS

Two million cells were washed 2 times with cold PBS and pelleted by centrifugation. Cell pellets were then flash frozen in liquid nitrogen and stored at -80°C until analysis. Quantification of (R)-2-HG in cell pellet was performed by LC negative electrospray ionization-MS/MS as described in the literature (Struys et al., 2004) with modifications. 0.3 mL 0.02% Triton-X100 PBS was added into each vial containing cell pellet, then the sample was sonicated for 20 s and repeated two additional times. The vials containing lysates were centrifuged at 14,000 rpm for 15 min. Protein concentration in supernatant was measured using Pierce BCA protein assay kit. 25 µL or 50 µL supernatant from each sample was added into different well of a 96-well plate triplicate. 25 µL (R)-2-HG standard solutions with (R)-2-HG concentrations at 13.1, 32.7, 81.9, 205, 512, 1280, 3200, 8000, 20000 and 50000 ng/mL were added into different wells of a 96-well plate. After adding 10 µL 5µg/mL 2-HG-d3 enantiomer (C/D/N Isotopes, Inc) as internal standard (IS), the mixture was dried by heated nitrogen. Dry residue was treated with 50 mg/mL freshly prepared diacetyl-L-tartaric anhydride in dichloromethane/glacial acetic acid (4/1 by volume) and heated (75°C 30 min). After drying with heated nitrogen, the residue was dissolved in 200 µL LC mobile phase A (see below) for analysis.

An Accela 1250 LC pump was used in this study. A sample volume of 70 µL was loaded onto an Xterra MS C18 analytical column (2.1x150 mm, 3.5 µm particle size) using a CTC-PAL autosampler at a flow rate of 0.3 mL/min. Isocratic separation was performed using water–acetonitrile (96.5:3.5 by volume) containing 125 mg/L ammonium formate

(pH adjusted to 3.6 by addition of formic acid) as mobile phase. The eluates were introduced into a triple quadrupole mass spectrometry, TSQ Vantage (ThermoScientific, San Jose, CA) by electrospray, at a flow rate of 0.3 mL/min. The TSQ Vantage was operated at a spray voltage of 3000 V, a capillary temperature of 360°C, sheath gas pressure of 50 and auxiliary gas pressure of 15. One SRM transition was recorded for both (R)-2-HG and IS, (R)-2-HG: Q1, 363.1 to Q3 147.1 (CE 11 eV); and IS, d3-(R)-2-HG: Q1, 366.1 to Q3 150.1 (CE 11 eV);. Resolution for Q1 and Q3 was set to 0.7. Thermo Xcalibur Quan Browser was used for data processing. Signal chromatographic peak area ratios between (R)-2-HG and d3-(R)-2-HG were established. Standard curves were constructed based on the signal peak area ratio against (R)-2-HG concentration (ng/mL) by linear regression using a weighting factor of 1/X.

Synthesis of (2-(2-(1H-benzo[d]imidazol-1-yl)-N-(3-fluorophenyl)acetamido)-N-cyclohexyl -2-(o-tolyl)acetamide and chiral purification (IDHi).

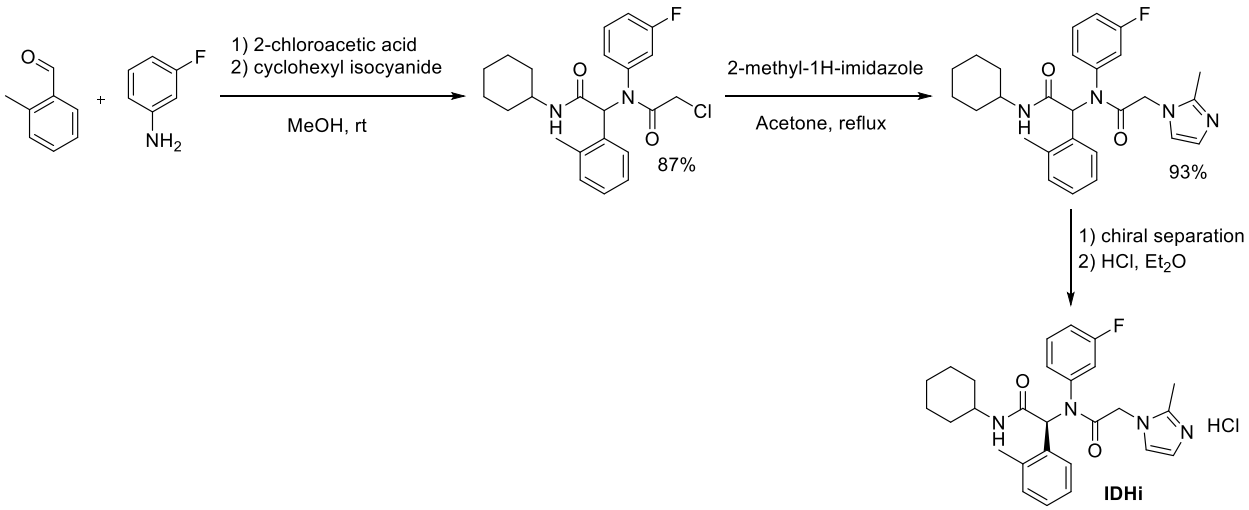

In a 1000 mL round-bottomed flask ortho-tolualdehyde (11.65 ml, 100 mmol) and 3-fluoroaniline (9.69 mL, 100 mmol) were mixed in 100 mL of MeOH. After stirring for 45 min at room temperature, 2-chloroacetic acid (9.52 g, 100 mmol) was added. After a further 15 min stirring at room temperature, cyclohexyl isocyanide (12.86 mL, 100 mmol) was added dropwise. The reaction mixture was stirred overnight at room temperature. A solid precipitated and was isolated by filtrating through a sintered glass funnel and the solid rinsed with cold MeOH then dried under vacuum to afford (2-chloro-N-(2-(cyclohexylamino)-2-oxo-1-(o-tolyl)ethyl)-N-(3-fluorophenyl)acetamide as a white powder (36.6 g, 87% yield). This white solid was dissolved in Acetone (300 mL) in a 1L flask. 2-methyl-1H-imidazole (31.51 g, 383.77 mmol) was added and the mixture was stirred overnight at reflux. Acetone was removed under reduced pressure and the compound was then further purified by chromatography on silica gel (in 3 batches, each with 330 g silica gel, CH_2Cl_2/MeOH : 100/0 to 90/10). 37.8 g of N-cyclohexyl-2-(N-(3-

fluorophenyl)-2-(2-methyl-1H-imidazol-1-yl)acetamido)-2-(o-tolyl)acetamide were obtained (93% yield).

^{1}H NMR (400 MHz, DMSO-d6) d: 8.02 (s, 1H), 7.84 (br s, 1H), 7.15-6.64 (m, 7H), 6.19 (s, 1H), 4.70-4.60 (m, 1H), 4.40-4.30 (m, 1H), 3.63-3.59 (m, 1H), 2.37 (s, 3H), 2.10 (s, 3H), 1.75-1.49 (m, 5H), 1.26-0.94 (m, 5H). MS: ES^+ (M + 1) = 463.5 m/z

The enantiomerically pure compound was isolated by separation of the racemate (6.5 g of racemate per injection, solubilized in a mixture of dichloromethane 40 mL / ethanol 40 mL / 100 mL heptane with sonication) using a chiral HPLC (Chiralcel, OD-I 20µm 350x76.5 mm column, UV 254 nm) and eluted with 70% heptane/30% EtOH at a flow rate of 350 mL/min. The two desired enantiomers (18.2 g and 17.5 g) were isolated as white powders. Assignment of stereochemistry was based on biological activity: within this chemotype, compounds with (*S*) configuration have been reported to be the active species against IDH1 R132H (Published patent application WO12009678). Therefore, Enantiomer 1 (biologically active vs IDH1 R132H and R132C, compound with the higher retention time on the chiral column) was assigned with the (*S*) configuration and designated **IDHi**, whereas Enantiomer 2 (inactive, smaller retention time) was assigned with the (*R*) configuration (Figure S1C). ^{1}H NMR and LCMS analyses were comparable to the racemic mixture.

For *in-vivo* use the hydrochloride salt was prepared : (*S*)-N-cyclohexyl-2-(N-(3-fluorophenyl)-2-(2-methyl-1H-imidazol-1-yl)acetamido)-2-(*o*-tolyl)acetamide (17 g) was loaded in a 1 L round bottom flask. Then hydrochloric acid in diethyl ether was added (1N, 500 ml). Suspension was stirred overnight and the white solid was isolated by

filtration, rinsed with diethyl ether and vacuum-dried. Compound activity was confirmed in biochemical and cellular assays to ensure that no epimerization occurred during the salt formation.

Biochemical and cellular characterization of IDHi

Reductive activity of mutant IDH1 (conversion of αKG to 2-HG) was monitored by LC-MS/MS as previously described (Deng et al., 2015). Briefly, assays were conducted in a 30 µL volume in a 384-well microplate (Corning 3824) in a buffer containing 50 mM HEPES, 150 mM NaCl, 20 mM $MgCl_2$, 1 mM DTT, and 0.005% Tween 20, pH 7.4. Inhibitors were incubated with enzyme and NADPH for 30 min, followed by initiation of the IDH1 reaction by addition of the substrate αKG. LC-MS/MS analysis was carried out on a TSQ Vantage Triple Stage Quadrupole mass spectrometer (Thermo Scientific) operated in electrospray negative ion mode. The mass spectrometer was coupled to a 1200 HPLC system (Agilent). Samples were injected using a PAL HTC autosampler (LEAP Technologies). Separation of 2-HG from other reaction components was achieved on a weak anion exchange column (20 mm x 2.1 mm, 5 µm; Thermo Biobasic) at a flow rate of 1.0 mL/min. Mobile phase B (0.2% NH_4OH in acetonitrile) was held at 90% for 15 s, before ramping mobile phase A (25 mM NH_4HCO_3 in water) from 10 to 75% over 30 s. Following this, mobile phase B was held at 90% for 18 s. The MRM transitions for 2-HG and $^{13}C_5$-2-HG (internal standard) were m/z 147 → 128 and m/z 152 → 134, respectively. Instrument parameters were: spray voltage, 2500 V; vaporizer temperature, 300 °C; sheath gas pressure, 60 liter/h; auxiliary gas pressure, 10 liter/h; capillary temperature, 350 °C; and collision energy, 30 V. Mass spectrometry data were acquired and processed using Xcalibur (Thermo Scientific). Peak area of 2-HG

was normalized using the peak area of the internal standard $^{13}C_5$-2-HG. IC_{50} values were derived using GraphPad Prism software.

To measure the effect of IDHi on 2-HG production in cells, Flp-In-T-Rex-293 cells (Life Technologies) were stably transfected with the inducible plasmid encoding R132H IDH1. For cell-based 2-HG measurements, IDH1 mutant-expressing cells were plated in growth media (DMEM, Life Technologies/10% Tet free FBS, Clontech) in the presence or absence of doxycycline (Clontech, 1 μg/ml) and cultured overnight. Compounds were added the following day and the cells were incubated for an additional 24 hours. An aliquot of the conditioned media was harvested and analyzed for 2-HG using the LC-MS/MS assay as described above. Cell viability was assessed using CellTiterGlo kit (Promega) according to the manufacturer's instructions.

2-HG and IDHi measurement in tumor tissues

Animals bearing MGG152 orthotopic xenografts were given IDH1i (400 mg/kg, 2X/day) or vehicle (20% captisol (CyDex), 5% dextrose in distilled water) by oral gavage for 5 days and then sacrificed for tumor tissue analysis. Tumor samples were spiked with 40 μL of 10 μM $^{13}C_5$-2-HG as internal standard and homogenized in 1ml 80% methanol/water using Precellys-24 with 2.8mm ceramic beads (5500 rpm for 2 x 30 s). The homogenate was centrifuged at 14000 rpm for 10 min and the supernatants were transferred into separate tubes. The methanol was removed by evaporation under vacuum and the residue was reconstituted in 2 mL water. Tissue concentration of 2-HG or inhibitor was quantified using LC-MS/MS as described above. The MRM transition for

IDHi was m/z 463 → 123. The peak area of 2-HG and IDHi was normalized using the peak area of the internal standard $^{13}C_5$-2-HG and tissue weight.

Metabolite profiling of cultured cells

Two million cells were washed 3 times with cold PBS and pelleted by centrifugation. Cell pellets were then flash frozen in liquid nitrogen and stored at -80°C until further processing. Metabolites were extracted by adding 1 ml of buffer (75% of 9:1 methanol/ chloroform in HPLC-grade H_2O) to the cell pellets. The lysates were incubated at 4°C for 20 min with shaking and cleared by centrifugation at 16,800 g for 5 min at 4°C. Two aliquots of supernatant were transferred to new Eppendorf tubes containing an acetonitrile/methanol (75/25, v/v) mixture. The samples were then dried-down using a SpeedVac and resconstituted with 100 ul of 50% acetonitrile in water for the analysis.

Profiling of amino acids, biogenic amines, nucleotides, neurotransmitters, vitamins and other polar metabolites was performed by LC-MS in positive ion mode. Profiling of TCA cycle intermediates, sugars and bile acids was performed by LC-MS in negative ion mode as previously described (Kimberly et al., 2013; Rhee et al., 2013). In brief, 10 µl of reconstituted sample was loaded onto either a 150 x 2.1 mm Atlantis HILIC column (Waters, Milford, MA) for positive mode analysis or a 50 x 4.6mm Synergi Polar-RP column (Phenomenex) for negative mode analysis using an HTS PAL autosampler (Leap Technologies, Carrboro, NC). The metabolites were separated using an Agilent 1200 Series HPLC system (Agilent Technologies, Santa Clara, CA) coupled to a 4000-QTRAP mass spectrometer (AB SCIEX, Foster City, CA). MultiQuant software v2.1 (AB

SCIEX, Foster City, CA) was used for automated peak integration and metabolite peaks were also assessed manually for quality of peak integration. LC-MS peak integration data of each sample were normalized to DNA content determined from a duplicate cell pellet. Heatmap was illustrated using JMP10 software.

Measurement of NAD+/NADH, NADP+/NADPH

To measure NAD+ and NADH quantitatively, NAD+/NADH Quatification Colorimetric Kit (BioVision Incorporated) was used according to manufacturer's recommendations. Briefly, $5x10^5$ cells, as indicated, were washed with cold PBS, and extracted in NADH/NAD extraction buffer by two cycles of freeze and thaw. To evaluate NAD+ change in tumor tissue, MGG152 cells were implanted into the striatum of SCID mice. Four weeks after implantation, mice were randomized to treatment with GMX1778 (250 mg/kg, n=3) or vehicle (n=3). 24 hr after treatment, mice were sacrificed and tumor tissues were harvested from brain. Protein concentrations were measured and used for normalization. NADt (NADH and NAD) and NADH signals were measured at OD 450nM (BIOTEK). NAD+ concentrations were calculated by subtracting NADH from NADt. Data were expressed as pmol/$1x10^6$ cells, pmol/mg protein, or normalized by DMSO control and presented as % change.

To evaluate qualitative values of NAD+, NADH, NADP+, and NADPH before and after Nampt inhibitors treatment, NAD/NADH-Glo™ Assay and NADP/NADPH-Glo™ Assay (Promega) were used according to manufacturer's recommendations. $1x10^5$ cells were lysed with 400 µl of PBS and then 400 µl of 0.2N NaOH with 1%

Dodecyltrimethylammonium bromide (Sigma-Aldrich) was added. To measure NAD+ and NADP+, equal volumes of 0.4N HCl were added to lysed cell sample (400 µl), followed by heating at 60C for 15 min. After incubation at room temperature for 10 min, 0.5M Trizma base buffer (200 µl, Sigma-Aldrich) was added. To measure NADH and NADPH, lysed cell sample (400 µl) were heated at 60C for 15 min, and then incubated at room temperature for 10 min, followed by adding equal volume of HCl/Trizma solution. Finally, samples were seed into 96 well plates and incubated with NAD/NADH-Glo and NADP/NADPH-Glo detection reagent for 30 min. Data were compared with DMSO treated cells and expressed as % control. To measure NADP+ and NADPH semiquantitatively, relative light unit/1x10^5 cells were used.

Western Blot analyses

Cells were lysed in radioimmunoprecipitation buffer (Boston Bioproducts) with a cocktail of protease and phosphatase inhibitors (Roche). 12.5 mg of protein was separated by 10% SDSPAGE and transferred to polyvinylidene difluoride membranes (EMD Millipore) by electroblotting. After blocking with 5% nonfat dry milk in TBST (20 mM Tris [pH, 7.5], 150 mM NaCl, 0.1% Tween20), membranes were incubated at 4C overnight with primary antibodies. After washing and incubation with horseradish peroxidase-conjugated secondary antibodies (Cell Signaling Technology), blots were washed, and signals were visualized with an ECL kit (Amersham Bioscience). Primary antibodies used were: anti-IDH1^{R132H} (Dianova), H3K9me2, H3K9me3 (Abcam), H3K4me3, H3K27me3, phospho-AMPK, phospho-Raptor, phospho-mTOR, phospho-S6 Ribosomal Protein, phospho-4E-BP1, phospho-ULK1 (ser555), phospho-ULK1 (ser757), LC3B,

GAPDH, and Actin (Cell Signaling Technology); NAMPT (Bethyl Laboratories), Naprt1 (Sigma-Aldrich), phospho-Atg13 (Rockland), and Vinculin (Thermo Scientific).

Immunohistochemistry

Tumor tissue specimens were fixed in 10% neutral-buffered formalin and embedded in paraffin. Hematoxylin and eosin staining was performed using the standard procedures. For immunohistochemistry 5-μm thick sections were deparaffinized, treated with 0.5% H_2O_2 in methanol to block endogeneous peroxidase, rehydrated, and heated for 25 minutes for antigen retrieval. Sections were blocked with serum, and incubated with primary antibody at 4C overnight. Next day, sections were washed in PBS, incubated with biotinylated secondary antibody for 60 min at room temperature, and then incubated with ABC solution (PK6200; Vectastain) for 30 min at room temperature. Finally, sections were stained with DAB (Dako) and counterstained with hematoxylin. Primary antibodies used were: anti-Ki-67 (1:125, Wako), Nestin (1:400, Santa Cruz), GFAP (1:400, Sigma-Aldrich), IDH1R132H (1:200, Dianova), H3K9me3 (1:400), and H3K9me2 (1:200, Abcam).

Measurement of cell viability, cytotoxicity, autophagy and apoptosis

TICs were dissociated and seeded into 96-well plates at 7,000-8,000 cells/well. Chemical inhibitors and/or NMN, NA, NAD+, decitabine, azacytidine, 3-MA were serially diluted and added to each well. After 48-120 hr, cell viability was measured by CellTiter-Glo (Promega).To evaluate Nampt inhibitors' efficacy, the IC50 values (the concentration of drug causing 50% viability of cells, not reached up to 10 μM) were

determined at 72 hr. To assess cell viability after IDH1i treatment, dissociated TICs were seeded into 96-well plates at 2,000-3000 cells/wells. 12-24hr later, cells were treated with 10 μM (TICs 9 days), 5 μM (30T, 3 days), or 1 μM (HT1080, 3 days) IDH1i, then cell viability (compared to DMSO control) was measured by CellTiter-Glo. To determine cytotoxicity, 7,000-8,000 cells were treated with DMSO, 12.5nM of FK866 or GMX1778, and the number of viable cells that excluded trypan blue was counted using TE2000-U inverted microscope (Nikon) at 48, 72, 96, 120, or 192 hr after treatment. To measure apoptosis, $1x10^5$ cells were seeded per well (12-well plates) and 24 hr later treated with inhibitors. After 48 hr incubation, cells were collected and stained with propidium iodide (PI) and APC-conjugated Annexin V (Annexin V apoptosis detection kit APC, eBioscience), and analyzed by an Accuri flow cytometer and the BD CSampler software (BD Biosciences). Caspase-3/7 activities were measured after 36 hr treatment with inhibitors by Caspase-Glo 3/7 Assay (Promega) as according to the manufacturer's recommendations.

Cell culture, creation of cell lines, genotyping and cell line fingerprinting

Glioblastoma TIC tumorsphere lines were generated from patient gliomas and were cultured as previously described (Wakimoto et al., 2009; Wakimoto et al., 2012; Wakimoto et al., 2014). Fresh surgical specimens were enzymatically dissociated and 2-5 x 10^4 cells were stereotactically implanted into the right striatum of the brains of 7-10-week-old female SCID mice. Mice were monitored for status twice per week and sacrificed when neurological deficits became significantly apparent. Brain tumors were removed for pathological studies and used to reestablish TIC neurosphere cultures,

which were then implanted into brains of new mice or used for in vitro assays. BT142, HT1080, U87, and SW1353 cells were obtained from American Type Culture Collection (ATCC). 30T and UACC257 were provided by Y.S. A431 cells were obtained from Sigma-Aldrich. Cells were cultured using EMEM (HT1080), RPMI-1640 (30T) and DMEM (U87, SW1353, and A431) supplemented with 10% fetal bovine serum (FBS), 4.5g/L glucose, L-glutamine, Penicillin-streptomycin-Amphotericin B, and sodium pyruvate. HCT116 lines (Parental, *IDH1*^{R132C}, and *IDH1*^{R132H}) and MCF10A cells were obtained from Horizon Discovery and cultured following manufacturer's specifications. NHA were obtained from ScienCell and were cultured with DMEM with 10% FBS.

To generate IDH1^{R132H} overexpressing GBM TIC lines, packaging 293T cells were transfected with lentivirus vector packaging plasmid DNA containing 6 μg of pLenti3.3/TR or pLenti6.3/TO/V5 containing IDH1^{R132H}, 4 μg of pCMV-dr8.2-dvpr, and 2 μg of pCMV-VSVG (ViraPower HiPerform T-Rex Gateway Expression System, Invitrogen) with ScreenFect (Wako). MGG18 TIC tumorspheres were infected with pLenti3.3/TR viral supernatant in the presence of polybrene (EMD Millipore, 8 μg/ml) for 6 hr, and selected with Geneticin (Roche; 150 μg/ml) for 14 days. Next, pLenti6.3/TO/V5 viral supernatant was added with polybrene (8 μg/ml) for 6 hr, and selected with Blasticidin (InvivoGen, 2 μg/ml) for 14 days. To induce expression of mutant IDH1, MGG18-IDH1-R132H cells were cultured with tetracycline (Sigma-Aldrich, 1 μg/ml) for 2 months. The Naprt1 overexpressing *IDH1* mutant GBM TIC line (MGG152-Naprt1) was generated using CCSB-Broad LentiORF-NAPRT Clone (GE Dharmacon), pCMV-dr8.2-dvpr and pCMV-VSVG. MGG152 TIC tumorspheres were infected with CCSB-Broad

LentiORF-NAPRT viral supernatant in the presence of polybrene (EMD Millipore, 8 μg/ml) for 6hr, and selected with Blasticidin (InvivoGen, 1 μg/ml) for 7 days. FK866, NAD+, NMN, NA, decitabine, azacytidine, and 3-MA were purchased from Sigma-Aldrich. GMX1778 was purchased from Cayman and Sigma-Aldrich.

Genomic PCR-based sequencing was used to sequence all coding exons of the *IDH1* and *IDH2* genes. PCR products were amplified from genomic DNA templates with Platinum Taq polymerase per manufacturer's protocol using intron-based primers spanning the expressed coding sequences and subsequently Sanger sequenced (Beckman Coulter Genomics). For cell line fingerprinting, DNA was amplified using the PowerPlex 16 HS System (Promega) as per manufacturer's protocol. Fragment analysis was then performed with the 3500xL Genetic Analyzer and GeneMapper Software (Applied Biosystems) following manufacturer's protocols.

Genome-Wide DNA methylation Analysis

Genome-wide methylation analysis was performed using the Illumina Infinium HumanMethylation450 BeadChip array. Genomic DNA is bisulfite treated using the Zymo EZ-96 DNA Methylation kit to convert unmethylated cytosines to uracil, leaving methylated cytosine intact. The converted DNA is then used as the starting material in an Infinium quantitative assay measuring levels of methylated cytosine versus unmethylated cytosine. The assay is a PCR independent assay, using 200-400 ng genomic DNA. The DNA is amplified using a whole genome amplification process. After fragmentation of the DNA, the sample is hybridized to 50-mer probes attached to the

Infinium Beadchips, stopping one base before the interrogated base. Single base extension is then carried out to incorporate a labeled nucleotide. Dual color (Cy3 and Cy5) staining allows the nucleotide to be detected by the iSCAN reader and is converted to genotype during analysis with the GenomeStudio analysis software (Illumina). The beta value (ß) is used to estimate the methylation level of the CpG locus using the ratio of intensities between methylated and unmethylated alleles Methylation values for each site are expressed as a ß value, representing a continuous measurement from 0 (completely unmethylated) to 1 (completely methylated). ß value= methylated allele intensity/(unmethylated allele intensity + methylated allele intensity).

Methylation-Specific PCR

Genomic and bisulfite-modified DNA was extracted using DNeasy Blood & Tissue and EpiTect Bisulfite kits (Qiagen). Methylation-specific PCR was performed in a two-step approach as described (Hegi et al., 2005).

Animal Efficacy Studies

To generate xenografts, $2x10^6$ of HT1080 cells (fibrosarcoma, $IDH1^{R132C}$) were implanted into the subcutaneous tissue of the right flank of 7-10-week-old female SCID mice (Taconic, n=12). When the maximum diameters of tumors reached 5mm, mice were randomized to treatment with intraperitoneal injections of FK866 (30 mg/kg, once a day; n=6) or normal saline (n=6) for 17 days. Tumor diameters were measured 2x/week using a digital caliper (Fisherbrand). Tumor volume was calculated using the

formula: tumor volume (mm3) = tumor length (mm) x tumor width (mm)2 x 0.5. HT1080 xenograft tumor tissues were harvested at day18. To generate orthotopic xenografts, 1-2x10^5 MGG152 glioma TIC cells were implanted into the right striatum of SCID mice as previously described (Wakimoto et al., 2014). Animals were administered IDH1i (400 mg/kg, twice per day) or GMX1778 (250 mg/kg, once per week) by oral gavage for the times indicated. Distilled water with 20% captisol (CyDex) and 5% dextrose (Sigma-Aldrich) was used as vehicle control. To evaluate the effect of long term culture with IDH1i, MGG152 cells were cultured with DMSO or 5 μM of IDH1i in neurosphere conditions in vitro, then, 1x10^5 cells were implanted intracerebrally as above at the indicated cell passage number. Mice were monitored for status everyday and sacrificed when neurologic deficits became significant. All mouse experiments were approved by the Institutional Animal Care and Use Committee (IACUC) of Massachusetts General Hospital and were performed in accordance with institutional and national guidelines and regulations.

SUPPLEMENTAL REFERENCES

Hegi, M., Diserens, A., Gorlia, T., Hamou, M., de Tribolet, N., Weller, M., Kros, J., Hainfellner, J., Mason, W., Mariani, L., et al. (2005). MGMT gene silencing and benefit from temozolomide in glioblastoma. N Engl J Med 352, 997-1003.

Kimberly, W. T., Wang, Y., Pham, L., Furie, K. L., and Gerszten, R. E. (2013). Metabolite profiling identifies a branched chain amino acid signature in acute cardioembolic stroke. Stroke; a journal of cerebral circulation 44, 1389-1395.

Published patent application WO12009678

Rhee, E. P., Ho, J. E., Chen, M. H., Shen, D., Cheng, S., Larson, M. G., Ghorbani, A., Shi, X., Helenius, I. T., O'Donnell, C. J., et al. (2013). A genome-wide association study of the human metabolome in a community-based cohort. Cell Metab 18, 130-143.

Struys, E. A., Jansen, E. E., Verhoeven, N. M., and Jakobs, C. (2004). Measurement of urinary D- and L-2-hydroxyglutarate enantiomers by stable-isotope-dilution liquid chromatographytandem mass spectrometry after derivatization with diacetyl-L-tartaric anhydride. Clinical chemistry 50, 1391-1395.